

Some Acoustic Features of Perforated Test Section Walls with Splitter Plates

Boris L. Medved*

National Research Council, Ottawa K1A 0R6, Canada

Transonic wind tunnels with perforated test section walls are generally known to have high noise levels. Calibration results of two large transonic wind tunnels [the Institute for Aeronautical Research (IAR) 1.5-m and T-38 1.5-m transonic wind tunnels] with walls that have slanted perforations with integral splitter plates have confirmed the effectiveness of splitter plates in suppressing edge-tone noise. However, as discovered in the T-38 wind tunnel, there are other wind tunnel components that generate flow disturbances. An experimental program, with the objective of identifying the sources of flow unsteadiness, has been performed in the T-38 wind tunnel. A comparison of the sources of flow unsteadiness between the IAR and the T-38 wind tunnels has been attempted.

Introduction

EXTENSIVE experimental investigations conducted both in wind tunnels and flight have shown that transition Reynolds number depends on the freestream static pressure fluctuation level.¹⁻⁴ Moreover, it has been found that the broadband noise levels below $M = 0.9$ can be very high in transonic test sections.

In general, ventilated transonic test sections with slanted holes generate higher static pressure fluctuations than slots. It has been found that resonant acoustic peaks, emanated from transonic walls, occur at frequencies on the order of a few kilohertz. However, Dougherty et al.,⁵ through an experimental investigation in a 1-ft transonic wind tunnel at Arnold Engineering Development Center (AEDC), have shown that the use of splitter plates inserted in the perforations can be an effective means of suppressing edge-tone noise.

Based mainly on that experience, two large wind tunnels have been built at the Institute for Aeronautical Research, the IAR and T-38, which have 1.5×1.5 m test sections whose walls have slanted perforations with integral splitter plates.^{6,7} These two facilities appear to be the only large transonic wind tunnels in the world having implemented splitter plates to suppress edge-tone noise. In such test sections that have been recently built (in the last six years), it was considered useful to investigate the impact of such a perforated wall configuration on the overall noise level in the test section. Also, there is very little data on turbulence and noise levels in existing blowdown facilities where a pressure regulating valve is considered a prime source of freestream disturbances to the test section flow.

The flow quality measurements in the T-38 wind tunnel have been done in two phases. The first phase has shown that other wind tunnel components generate flow disturbances. The measurements in this wind tunnel have also shown the existence of acoustic resonant peaks in the low frequency range, below 50 Hz at all subsonic Mach numbers.

In the second phase, an experimental program was performed to try to identify the origin of these flow disturbances.

Three possible sources of low frequency disturbances were indicated during phase one. These were the pressure regulating valve, the test section diffuser, and the perforated test section walls. Although the test section walls were judged to be the least probable source of the low frequency static pressure fluctuations, a new series of measurements with solid test section walls were carried out.

To prevent possible flow disturbances generated in the test section diffuser from propagating upstream into the test section, a two-dimensional choke system was designed, built, and installed at the end of the test section. This two-dimensional choke was located upstream of the model strut, forming a sonic surface close to the leading edge of the strut. Location of the choke system was dictated by practical reasons. The two flaps were attached to the schlieren window blanks on the flexible nozzle sidewalls. Moving the flaps further downstream would have required major modifications to the wind tunnel, which were considered unacceptable.

Some basic static pressure fluctuation comparisons between the IAR and the T-38 wind tunnels will be presented in the paper. These two transonic wind tunnels have almost identical test section wall configurations. However, because of differences in transonic Mach number control, the test section diffuser and plenum chamber geometries are different.

Test Description—Phase I

Two probes were used to measure the static pressure fluctuations in the test section and settling chamber. The first one, the 20-deg cone-cylinder probe shown in Fig. 1, was designed

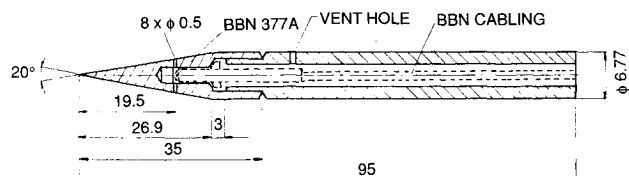


Fig. 1 20-deg cone-cylinder probe.

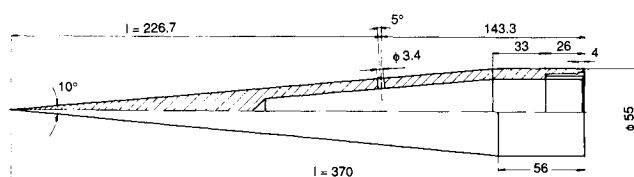


Fig. 2 10-deg cone probe.

Presented in part as Paper 90-1418 at the AIAA 16th Aerodynamic Ground Testing Conference, Seattle, WA, June 18-20, 1990, and as Paper ICAS 92-3.8.3 at the 18th International Council of the Aeronautical Sciences Congress, Beijing, China, Sept. 20-25, 1992; received Aug. 18, 1992; revision received March 1, 1993; accepted for publication March 2, 1993. Copyright © 1993 by Boris L. Medved. Published by the American Institute of Aeronautics and Astronautics, Inc., with permission.

*Research Officer, Institute for Aeronautical Research, High Speed Aerodynamic Laboratory, Montreal Road.

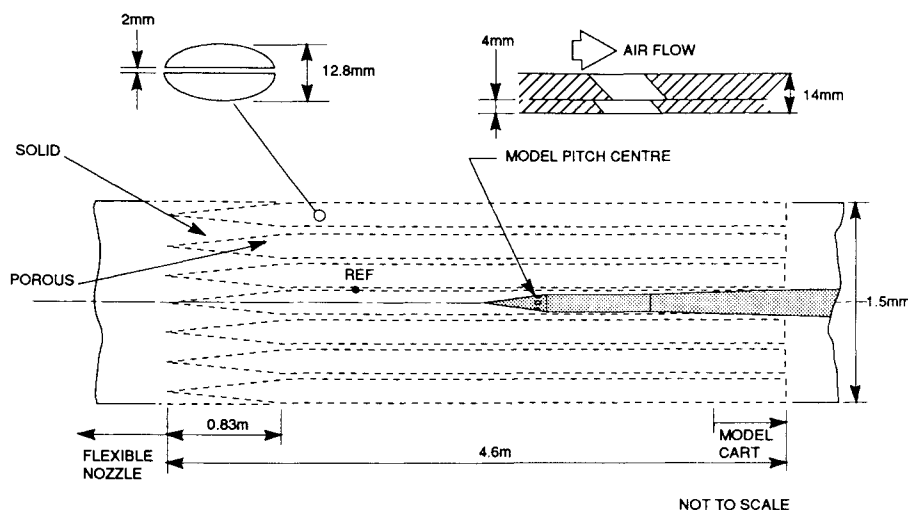


Fig. 3 Perforated test section geometry with splitter plates.

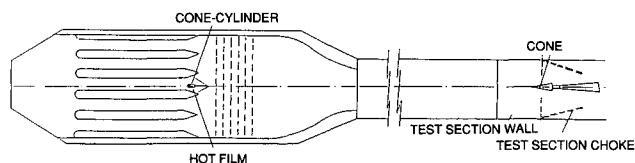


Fig. 4 Sketch of T-38 wind tunnel and measuring locations.

to sense high-frequency edge-tone noise without the complication of probe-induced turbulent boundary-layer noise. A piezoelectric pressure transducer, BBN Model 377A, was used to sense fluctuating pressures. The second probe, the 10-deg cone probe shown in Fig. 2, was a scaled version of the well-documented AEDC cone probe. The second probe was chosen as a check for the first one. The BBN transducer was flush mounted to the cone surface. Both probes were kept aligned with the model pitch center, as shown in Fig. 3. Although there was some concern about the cone-cylinder probe regarding modified frequency response and formation of flow separation bubble due to the probe shoulder, results from the two probes showed very good agreement.

The layout of the perforated test section wall configuration with the inserted splitter plates in the holes is also presented in Fig. 3. In the T-38 wind tunnel, slanted perforations are 12.8 mm in diameter. The splitter plates are 2 mm thick. Test section porosity can be varied from 1.5 to 8%. For comparison, in the IAR wind tunnel, the diameter of the perforations is 12.7 mm, with the thickness of the splitter plates at 1 mm. To better accommodate transonic testing, porosity can be varied from 0.5 to 6%.

Tests were carried out over the Mach number range from 0.4 to 1.4, primarily at a blowing pressure of 3 bars.

A few runs were performed at higher blowing pressures to investigate the influence of Reynolds number. The optimum porosity distribution with Mach number for the T-38 transonic test section was used for all of the runs.⁸ Other than optimum porosity settings were used in a few runs to investigate porosity effect on the noise level. Two repeat runs at $M = 0.7$ and 1.0 were done. Repeatability with these flow conditions was excellent.

Test Description—Phase II

Noise and turbulence levels were measured during this calibration phase in both the settling chamber and test section, as shown in Fig. 4. The measurements were made with and without the new test section choke configuration.

An instrumentation schematic showing the noise and turbulence measuring equipment as well as the data reduction system is presented in Fig. 5.

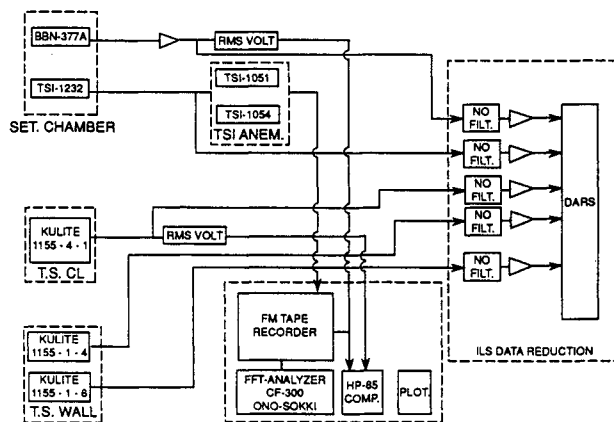


Fig. 5 Instrumentation schematic in T-38 wind tunnel.

The noise transducer signals were fed to rms voltmeters (10 Hz–20 kHz). All signal outputs were recorded in parallel to a NAGRA NTA4 analog tape recorder (0–10 kHz) with an accuracy of ± 0.2 dB. Spectral analysis was accomplished using a two channel digital FFT HP 3562A analyzer (0–100 kHz) with an accuracy of 0.15 dB, and using the software package ILS installed on the VAX 11/780. The sampling rate of the unfiltered signals was 4000 Hz. The noise transducers were fully calibrated prior to the test using B&K 4221 calibration equipment. In addition, the transducers were frequently checked during the test using a B&K Pistonphone at $SPL = 124 \pm 1$ dB and $f = 250$ Hz.

The test Mach number range with the conventional second throat configuration was from 0.3 to 0.9; with the test section choke configuration it was from 0.5 to 0.8. The blowing pressure for all test conditions was 3 bars.

Results and Discussion

The rms voltmeter results from the first calibration phase, in C_p vs Mach number form, are shown in Fig. 6.

Two runs were performed with porosity settings other than the optimum to determine the effects of porosity on the noise level. These two runs were at $M = 1$ ($\tau = 4\%$ compared to $\tau_{opt} = 1.5\%$) and at $M = 0.67$ ($\tau = 1.5\%$ compared to $\tau_{opt} = 4\%$). No change, either in the broadband noise level or in the frequency spectra distribution, was noticed.

To determine Reynolds number effect on the noise level, three additional runs with different blowing pressure were done: 1) $M = 0.65$, $p_0 = 2$ and 5 bar, and 2) $M = 0.7$, $p_0 = 5$ bar. No Reynolds number influence could be observed on the

noise level or on the sound energy distribution in the frequency plane.

Characteristic frequency spectra for the typical low subsonic Mach number of 0.62 are shown in Fig. 7. As seen from the spectrum, periodic components are concentrated in the low frequency domain, below 50 Hz (see also the spectrum with 6 kHz frequency range). There is no change in discrete frequency locations in Mach number interval (0.5–0.75).^{9,10} If the dominant frequency of $f = 37$ Hz is interpreted to be an acoustic half-wave resonance, the converted characteristic length would be 4.6 m. This is the length of the test section (including perforated fingers) as well as the length of the

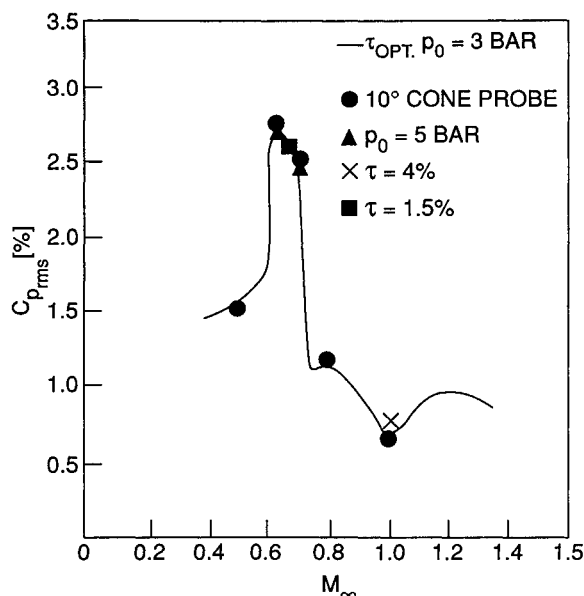


Fig. 6 Broadband noise level in T-38 wind tunnel.

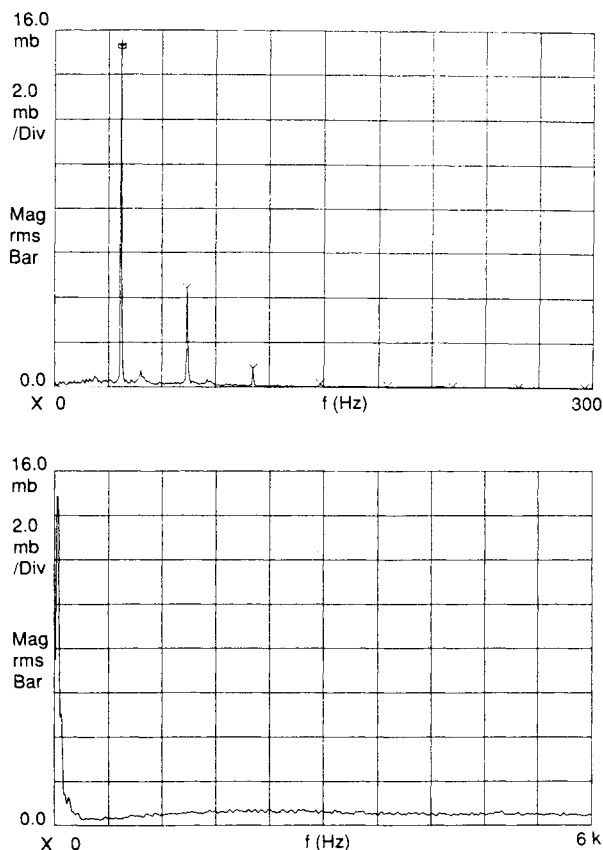


Fig. 7 Frequency spectra at $M = 0.62$ —perforated walls.

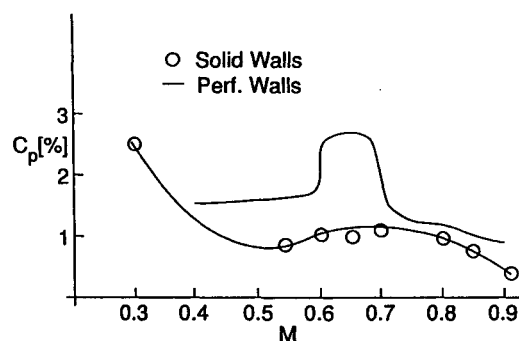


Fig. 8 Static pressure fluctuations with perforated and solid walls in T-38 wind tunnel.

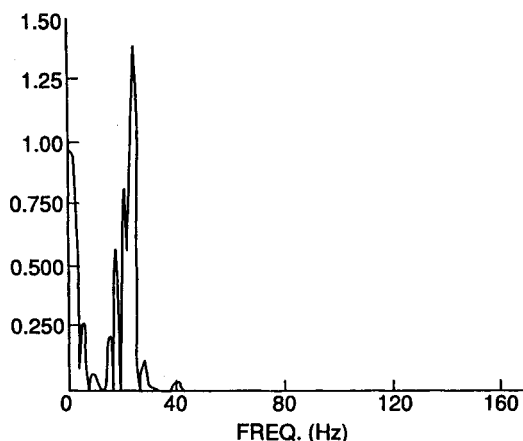


Fig. 9 Frequency spectrum at $M = 0.6$ —solid walls.

plenum chamber. This result indicates that the acoustic signals are caused by the flow exciting a resonance mode in the plenum chamber.

A comparison of the perforated and solid test section wall configurations for the T-38 wind tunnel is given in Fig. 8. The noise level in the test section with the solid walls is significantly reduced, confirming the existence of resonant flow conditions in the plenum chamber. Even with the solid wall test section configuration, part of the model cart of 0.5 m in length remains perforated at all times (see Fig. 3). During this investigation porosity of this perforated area was set to 4%.

The frequency spectrum at $M = 0.6$ with the solid test section walls is shown in Fig. 9. A dominant peak in the low frequency range is present at 24.8 Hz. This frequency could correspond to the distance between the end of the flexible nozzle and the choke system. This dominant frequency was not observed with the perforated test section, but it could have been masked by more dominant acoustic energy peaks.

The broadband noise level at the test section centerline for the two different choke configurations is shown in Fig. 10. The results indicate no noticeable difference in the noise levels in the Mach number range from 0.5 to 0.65. However, in the Mach number range from 0.65 to 0.8, the difference in the noise levels is quite significant, with the noise level lower in the choked test section by about 1 to 0.5%. This difference demonstrates the effectiveness of the sonic surface in preventing flow disturbances generated in the diffuser from propagating upstream into the test section.

Frequency spectra at two different Mach numbers with the test section choke system are given in Figs. 11 and 12. The acoustic energy distribution does not change significantly with Mach number. The resonant acoustic peak noticed with the conventional choke remained at the same frequency of 24.8 Hz but with significantly reduced amplitude. Reduction in amplitude appears to confirm the preceding indication that the

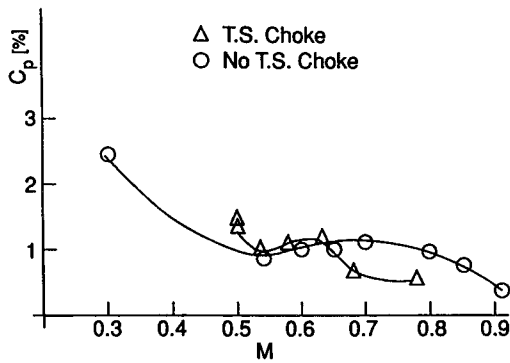


Fig. 10 Static pressure fluctuations with different choke configurations.

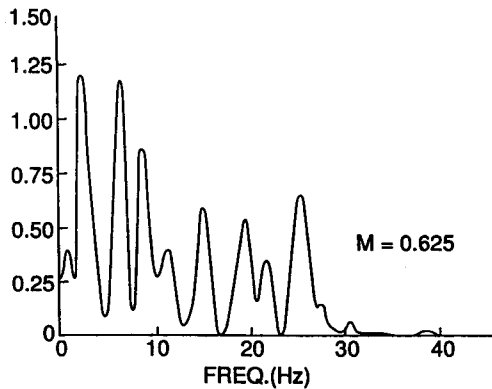


Fig. 11 Frequency spectrum with solid walls and test section choke, $M = 0.625$.

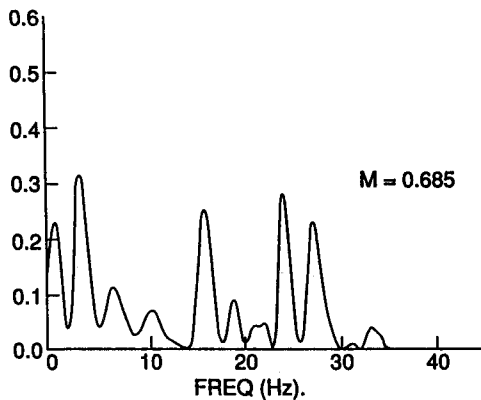


Fig. 12 Frequency spectrum with solid walls and test section choke, $M = 0.685$.

test section choke is quite effective in reducing upstream propagating acoustical disturbances.

A comparison of the noise levels at the test section sidewall location for the two choke configurations is given in Fig. 13. The conventional choke configuration has slightly better characteristics in terms of the noise level. Comparison of Figs. 10 and 13 suggests an upstream propagation of the acoustic disturbances, which begins to occur at flow conditions of about $M = 0.65$. The upstream propagating acoustic wave is pronounced at the centerline location, but attenuated at the test section wall downstream location. Flow disturbances propagating downstream dominate up to a Mach number of about 0.65, with the upstream propagating acoustic disturbances becoming more dominant at the higher Mach numbers.

The turbulence level in the settling chamber is presented in Fig. 14. The hot film probe was located between the acoustic baffles and the first of the six screens in the settling chamber.

The turbulence level recorded upstream of the first screen is reasonably low, considering the highly unsteady flow conditions existing downstream of the pressure regulating valve. Several runs were made with the probe in the settling chamber located in two alternate positions, about 2 m to both left and right of the centerline. The results showed no significant variations of the turbulence level among the three different probe locations, indicating a very good spatial turbulence distribution in the settling chamber. This uniformity appears to be a very good indication that the flow conditioning devices between the control valve and the first screen have been chosen properly. These devices consist of three wide angle diffuser baffles, with open area ratios of 25.5, 27.5, and 36.9%. In addition, four plus two halves parallel acoustic silencers are installed downstream of the last diffuser baffle.

The turbulence level in the test section measured with the two choke configurations is shown in Fig. 15. As expected, the two different choke configurations do not effect the turbulence level. However, the turbulence level in the test section is very high compared with that in the settling chamber, considering that the contraction ratio for the wind tunnel is 8.7:1. A preliminary analysis, not shown here, suggests that excessive

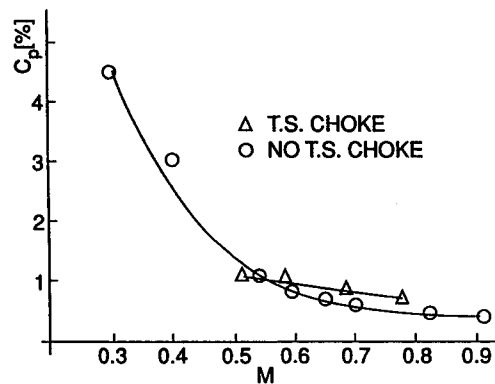


Fig. 13 Static pressure fluctuations at test section wall.

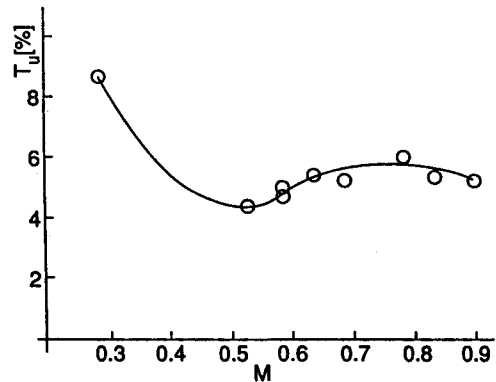


Fig. 14 Turbulence level in settling chamber.

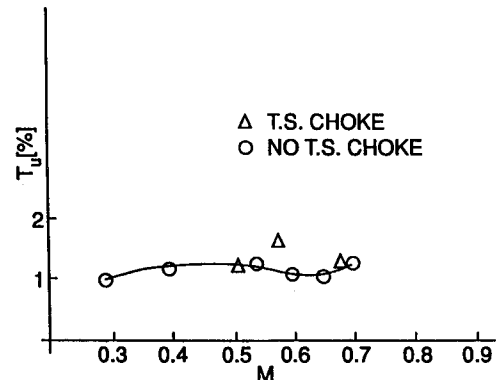


Fig. 15 Turbulence level in test section.

screen solidity along with the wake turbulence from the parallel acoustic silencer is a likely source of the higher turbulence level in the test section. The solidity of the downstream screen is 0.52, whereas 0.43 is generally considered the safe maximum.

Figure 16 shows a comparison of the freestream static pressure fluctuations at the four different wind tunnel locations with the conventional (second throat) choke configuration. A high level of the upstream traveling acoustic disturbances is noticeable at the higher Mach numbers.

The same type of comparison, but with the test section choke configuration, is given in Fig. 17. The test section choke is shown to be effective at the higher Mach numbers since it lowers the noise level in the test section at these flow conditions. However, Figs. 16 and 17 show the test section choke to be ineffective at the lower Mach numbers at the downstream sidewall location indicative of the downstream nature of the acoustic wave propagation.

The noise levels, as a function of Mach number, with both conventional and test section choke configurations are given in Fig. 18. The noise level in the settling chamber appears to be insensitive to Mach number, but the level at the test section location centerline is significantly affected by the upstream propagating wave for flow conditions above $M = 0.65$. This effect is significantly attenuated by the test section choke. Finally, at the sidewall transducer location, the noise level appears to be unaffected by the upstream propagating waves.

Some basic noise level comparisons between the IAR and the T-38 tunnels will be given here. It is of interest to compare the noise characteristics of these two wind tunnels because of the similarities between them with regard to wind tunnel type, test section size, and test section wall configuration.

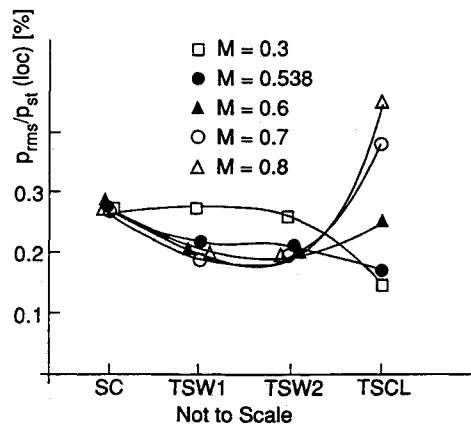


Fig. 16 Noise levels at different wind tunnel locations.

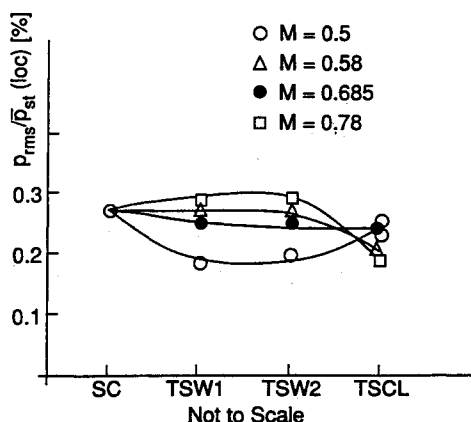


Fig. 17 Noise levels at different wind tunnel locations with test section choke.

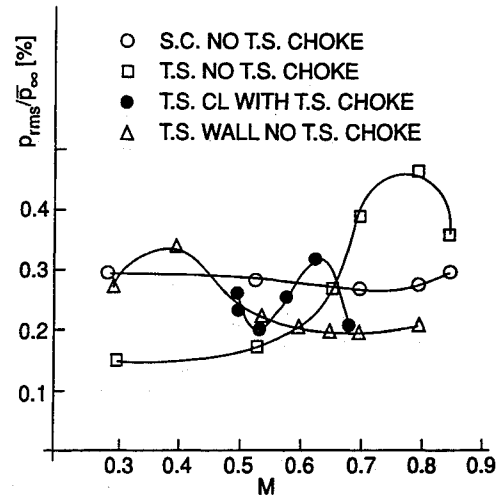


Fig. 18 Static pressure fluctuations with different choke configurations.

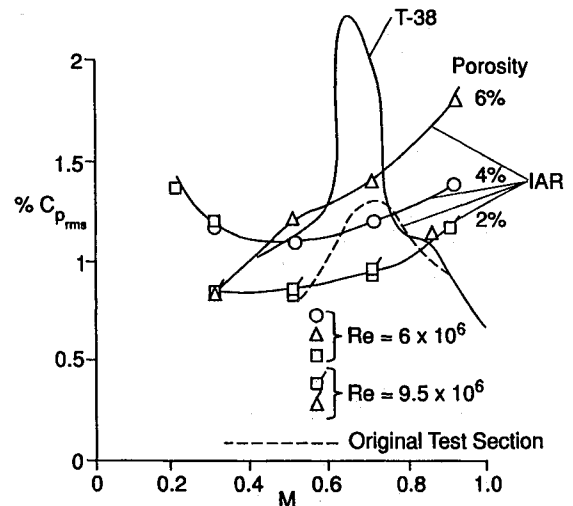


Fig. 19 Static pressure fluctuation level comparison between IAR and T-38 wind tunnels.

Figure 19 shows the noise levels in the three-dimensional test sections of the two wind tunnels. The noise level in the T-38 wind tunnel was measured at 4% porosity for Mach numbers up to 0.9. There is no similarity in the noise characteristics between the two wind tunnels at 4% porosity. Beyond $M = 0.7$, the two different test section diffusers influence the noise level differently in the same type of the test section. The difference in the test section diffusers is due to different design in controlling the Mach number at transonic speeds. Mach number control in the T-38 wind tunnel is achieved by using forced mass outflow through two blowoff valves. In the IAR wind tunnel, Mach number is controlled by re-entry flaps allowing direct flow communication between the plenum chamber and diffuser. In addition, in the IAR wind tunnel, a translating choke system consisting of two vertically translating fingers has been involved for Mach number control. This second throat in the diffuser is located far downstream of the test section (~ 6 m). The choke system in the T-38 wind tunnel, consisting of four flaps, is attached to the model support strut; therefore, it is closer to the test section (~ 3 m). The total diffuser angle in the T-38 wind tunnel is 6.2 deg.

The sharp degradation in the flow quality of the T-38 wind tunnel in the Mach number range from 0.6 to 0.7 can be attributed to the occurrence of resonant conditions in the plenum chamber. As seen in Fig. 19, no similar peak exists in the IAR wind tunnel test section.

Concluding Remarks

The centerline broadband noise measurements in the T-38 wind tunnel show similar characteristics of $C_{p_{rms}}$ vs Mach number to other large transonic wind tunnels.

The splitter plates have successfully suppressed generation of edge-tone noise, resulting in low broadband noise level in the transonic flow regime.

The resonant frequencies at all flow conditions are located in the low frequency domain (below 50 Hz). This feature is quite different from other large transonic test section configurations where the resonant peaks are located at higher frequencies (up to several kilohertz).

It was found that the Reynolds number and the test section wall porosity had no influence on either broadband noise level or noise energy distribution in the frequency plane.

Low frequency flow disturbances, previously found with the perforated test section configuration, were also shown to be present with the solid walls configuration.

The two-dimensional choke fitted at the downstream end of the test section was shown to be very effective in preventing the diffuser originating noise from propagating upstream into the test section for the flow conditions above Mach 0.65.

The sharp degradation in the flow quality of the T-38 wind tunnel in the Mach number range from 0.6 to 0.7 can be attributed to the resonant conditions in the plenum chamber.

A comparison of the noise levels between the IAR and T-38 wind tunnels shows that the different diffuser geometries produce different noise characteristics even though the test section configurations are similar.

References

- ¹Dougherty, N. S., and Steinle, F. W., "Transition Reynolds Number Comparisons in Several Major Transonic Tunnels," AIAA Paper 74-627, 1974.
- ²Dougherty, N. S., and Fisher, D. F., "Boundary Layer Transition on a 10 degree Cone—Wind Tunnel and Flight Data Correlation," AIAA Paper 80-154, 1980.
- ³Dougherty, N. S., "Boundary Layer Transition Correlation on a Slender Cone in Wind Tunnel and Flight for Indications of Flow Quality," Arnold Engineering Development Center, AEDC-TR-81-26, 1982.
- ⁴Elsenaar, A., "Reynolds Number Effects on Wind Tunnel Environment," AGARD-AR-224, 1988.
- ⁵Dougherty, N. S., Anderson, C. F., and Parker, R. L., "An Experimental Study on Suppression of Edgetones from Perforated Wind Tunnel Walls," AIAA Paper 76-50, 1976.
- ⁶Medved, L. B., and Elfstrom, G. M., "The Yugoslav 1.5 m Transonic Blowdown Wind Tunnel," AIAA Paper 86-0746, March 1986.
- ⁷Ohman, L., and Brown, D., "Performance of the New Roll-In-Roll-Out Transonic Test Sections of the NAE 1.5 m x 1.5 m Blowdown Wind Tunnel," International Council of the Aeronautical Sciences, Paper ICAS-90-6.2.2, Sept. 1990.
- ⁸Elfstrom, G. M., Medved, B., and Rainbird, W. J., "Wave Cancellation Properties of a Splitter-Plate Porous Wall Configuration," *Journal of Aircraft*, Vol. 26, No. 10, 1989, pp. 920-924.
- ⁹Medved, L. B., Vitic, A., and Elfstrom, G. M., "Broadband Noise Measurement in the Transonic Test Section of the VTI T-38 Wind Tunnel," AIAA Paper 90-1418, June 1990.
- ¹⁰Medved, L. B., and Vitic, A., "Generation of Flow Disturbances in Transonic Wind Tunnels," International Council of the Aeronautical Sciences, Paper ICAS-92-3.8.3, Sept. 1992.

Proceedings from the 18th Congress of the International Council of the Aeronautical Sciences

September 20-25, 1992 • Beijing, People's Republic of China

The ICAS '92 conference proceedings offer 274 exceptional papers, representing work in all branches of aeronautical science and technology. Conveniently packaged in two volumes, you will find up-to-date information on the following topics: air traffic control • performance and trajectory optimization • turbomachinery and propellers • CFD techniques and applications • maintenance systems, subsystems and manufacturing technology • lighter than air • engine/airframe integration • aircraft design concepts • passenger and crew safety • aeroelastic analysis • performance, stability and control • navigation • fault tolerant systems • fatigue • structural dynamics and control • aerodynamics • noise • combustion • wind tunnel technology • structural testing • high incidence and vortex flows • impact behavior of composites • aircraft operations and human factors • system safety and dynamics • fatigue and damage tolerance • hypersonic aircraft • avionics • supersonic and hypersonic flow • crew activity and analysis • simulators and man-machine integration • CAD/CAM and CIM, and much more

1992, 2-vol set, 2,200 pp, paper, ISBN 1-56347-046-2, AIAA Members \$130, Nonmembers \$150, Order #: 18-ICAS

Place your order today! Call 1-800/682-AIAA



American Institute of Aeronautics and Astronautics

Publications Customer Service, 9 Jay Gould Ct., P.O. Box 753, Waldorf, MD 20604
FAX 301/843-0159 Phone 1-800/682-2422 9 a.m. - 5 p.m. Eastern

Sales Tax: CA residents, 8.25%; DC, 6%. For shipping and handling add \$4.75 for 1-4 books (call for rates for higher quantities). Orders under \$100.00 must be prepaid. Foreign orders must be prepaid and include a \$20.00 postal surcharge. Please allow 4 weeks for delivery. Prices are subject to change without notice. Returns will be accepted within 30 days. Non-U.S. residents are responsible for payment of any taxes required by their government.